

# SYNGENETIC STRONTIUM ORE DEPOSITION AT THE BASE OF ASMARI FORMATION, BANGESTAN ANTICLINE, BEHBAHAN, IRAN

F. Moore and M. Jami

*Geology Department, College of Sciences, Shiraz University, Shiraz,  
Islamic Republic of Iran*

## Abstract

Detailed petrographic, geochemical and strontium isotope studies, combined with field observation and microfacies investigations indicate that syngenetic celestite at the base of Asmari Formation at the Bangestan anticline, Behbahan region, was deposited directly from Tertiary seawater in an intrasupratidal to supratidal environment. During diagenesis, the precipitated celestite underwent several textural and mineralogical modifications, the most important of which was the formation of diagenetic crystallization rhythmites. Fluid inclusion geothermometry and FTIR analyses suggest that the fluid medium, in which recrystallization of the celestite took place, was among other constituents rich in immature hydrocarbons. It is demonstrated that the celestite concretions were subjected to several low temperature thermal events, the maximum of which did not exceed 255°C.

## Introduction

There are twenty-seven known strontium minerals, of which only celestite is commercially significant. Celestite is generally converted to carbonate for use in glass and related industries and to nitrate for use in pyrotechnics. However, the largest use of strontium is in television picture tubes because it blocks X-ray emission from the picture tube during operation of the television set.

Great Britain was the principal producer of celestite until 1970. In the decade from 1960 to 1970, almost 90 percent of the world's celestite output was from the famous Bristol ore field [31]. However, during the last two decades the situation has completely changed. The world production of celestite grew by a factor of three in the years between 1973 and 1978 from 50000 metric tons to 150000 metric tons [28]. The data published by the U.S. Bureau of Mines for 1993 indicate that Mexico with an annual production of approximately 71903 metric tons is the leading producer of strontium minerals, and Great Britain with 1000 tons

production has been relegated to the fifth place following Turkey, Iran and Spain. Presently, almost half of the world's production of strontium ore comes from Mexico. United States consumes almost 75 percent of the world production. Other major consumers include Japan and Europe.

Brodtkorb [4] in a classical study of celestite ore fields worldwide noticed the striking geological similarities of these deposits. She concluded that in the exogenous cycle, celestite always precipitates in a certain facies of the evaporite sequence, invariably related to carbonates and gypsum. Chabou *et al.* [7] suggest that celestite is a good paleogeographic and climatic indicator for arid and semi arid regions.

Iran is located in the so-called celestite belt of western Asia [25]. There are two known celestite occurrences in Iran. The first is located in central Iran and includes the Nakhjir celestite deposit. The second is located in the Zagros mountain range of western Iran and includes the more recently exploited Likak deposit.

**Keywords:** Bangestan anticline; Celestite; Syngenetic

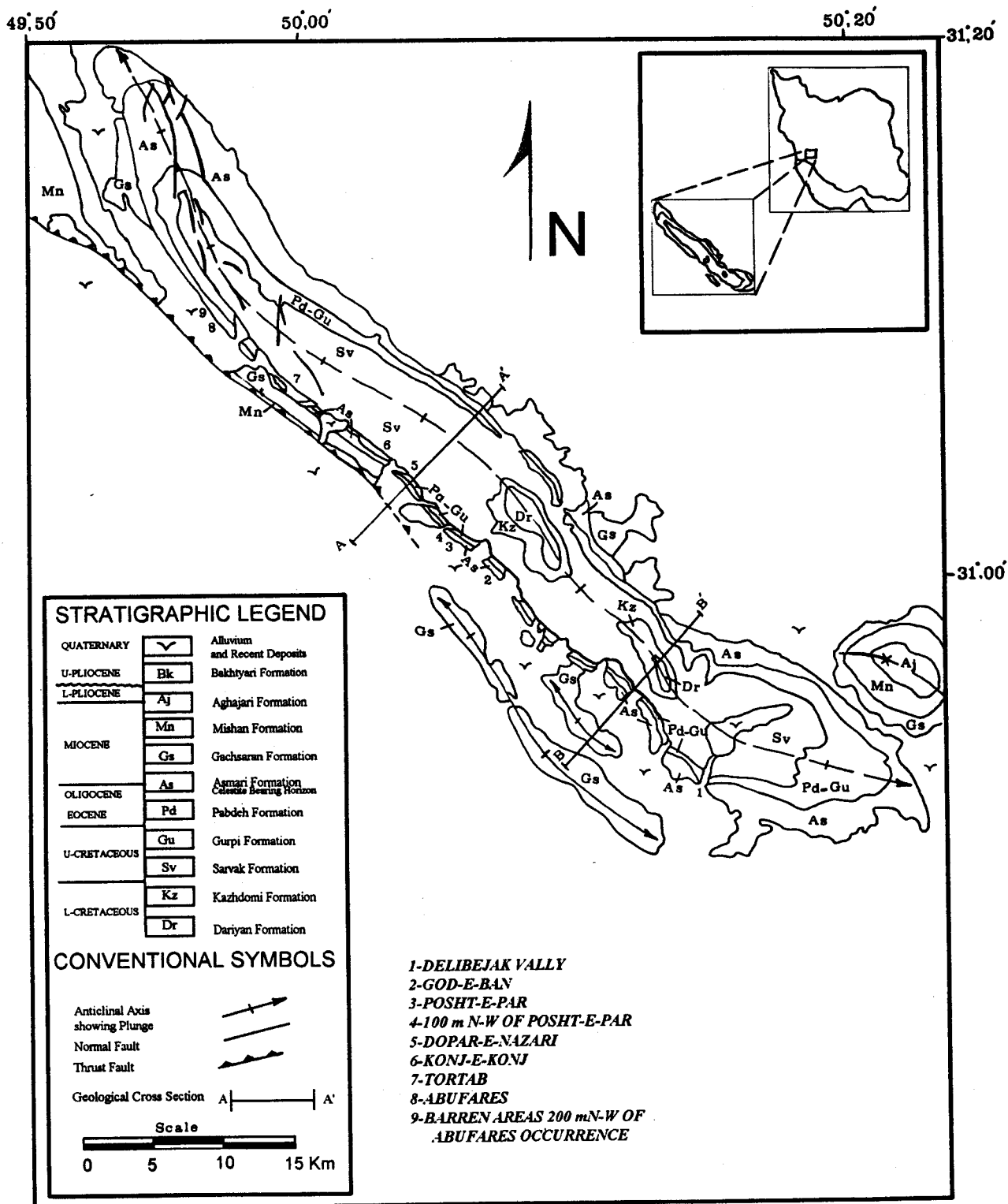


Figure 1. Geological map of Bangestan anticline (modified from Jami [10])

Previous work on the strontium deposits of Iran is confined to a sole publication by Schiebel [27] on Nakhjir deposit. According to Schiebel, the Nakhjir deposit of central Iran was formed by an evaporate process of enrichment. Celestite is associated with gypsum, anhydrite and gypsyferous marls, and one to two percent barite is present at the top of the celestite layers.

So far two celestite horizons have been reported in the Zagros mountain range, both occurring in the Bangestan anticline northwest of Behbahan city. The richer and younger seam, which is Miocene in age and includes the famous Likak deposit, occurs in evaporites of Gachsaran Formation. The older horizon is late Oligocene-early Miocene and occurs at the evaporitic base of Asmari Formation [17, 26].

The main aim of the undertaken study is the determination of overall geological conditions of the celestite deposition at the base of Asmari Formation in Bangestan anticline and the investigation of post depositional changes in these deposits.

### Regional Setting

The Bangestan anticline with 75 km length and 10 km width, lies within the southern margin of the Zagros Mountain Range (ZMR) in an area generally known as "simply folded belt" (30°, 48' to 31°, 15' N & 49°, 52' to 50°, 22' E). The detailed geology of ZMR is described by James and Wynd [16], Stocklin [29], Falcon [12], Alavi [1] and more recently by Darvishzadeh [9]. The trend of the Bangestan anticline is similar to the ZMR general trend i.e.

northwest-southeast.

The exposed Formations from oldest to youngest are the calcareous Dariyan Formation (Neocomian-Aptian), marly Kazhdomi Formation (Albian), calcareous Sarvak Formation (Cenomanian-Turonian), shaly Gurpi and Pabdeh Formations (Santonian-Companian), calcareous Asmari Formation (Oligocene-Miocene), evaporitic Gachsaran Formation (Miocene), calcareous Mishan Formation with marly intercalations (Miocene), arenaceous Aghajari Formation (Pliocene), and conglomeratic Bakhtyari Formation (Pliocene). The contacts between all these formations are conformable except for the angular unconformity between Aghajari and Bakhtyari Formations.

The Bangestan anticline is structurally very little disturbed. However, contrasting response of shaly, evaporitic and calcareous formations to tectonic forces has caused huge slides and numerous overturns to occur. Several small normal faults of local importance also occur in the anticline. The faults are mostly concentrated in the northern segment of the anticline reflecting their relation to Dailam-Aligodarz lineament [26]. A rather large high angle thrust fault in the southern flank of the anticline overthrusts the Mishan Formation over Aghajari Formation for at least 1 km. Figures 1 and 2 depict the main geological features of the Bangestan anticline. Figure 1 clearly shows that the axis of the doubly plunging anticline curves at both ends towards the north. The curving is more prominent at the northern end where the trend of the axis changes from N 70°W in the center of the anticline to N 10° W. The Pasadonian Orogeny of early Pliocene and the ensuing

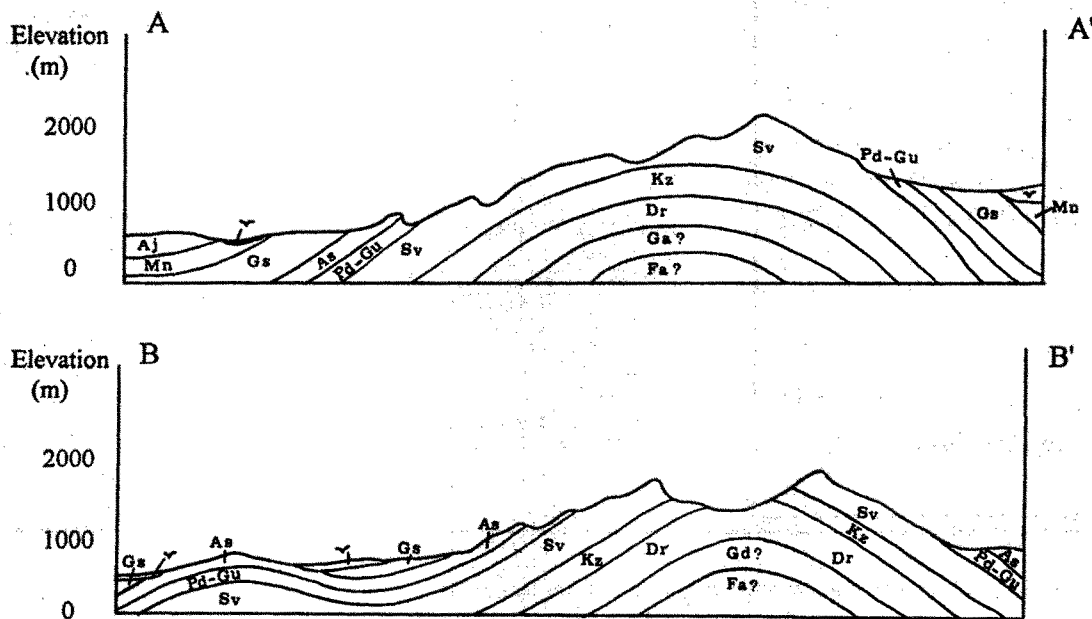


Figure 2. Geological cross sections across lines AA' and BB' (vertical exaggeration ~0)

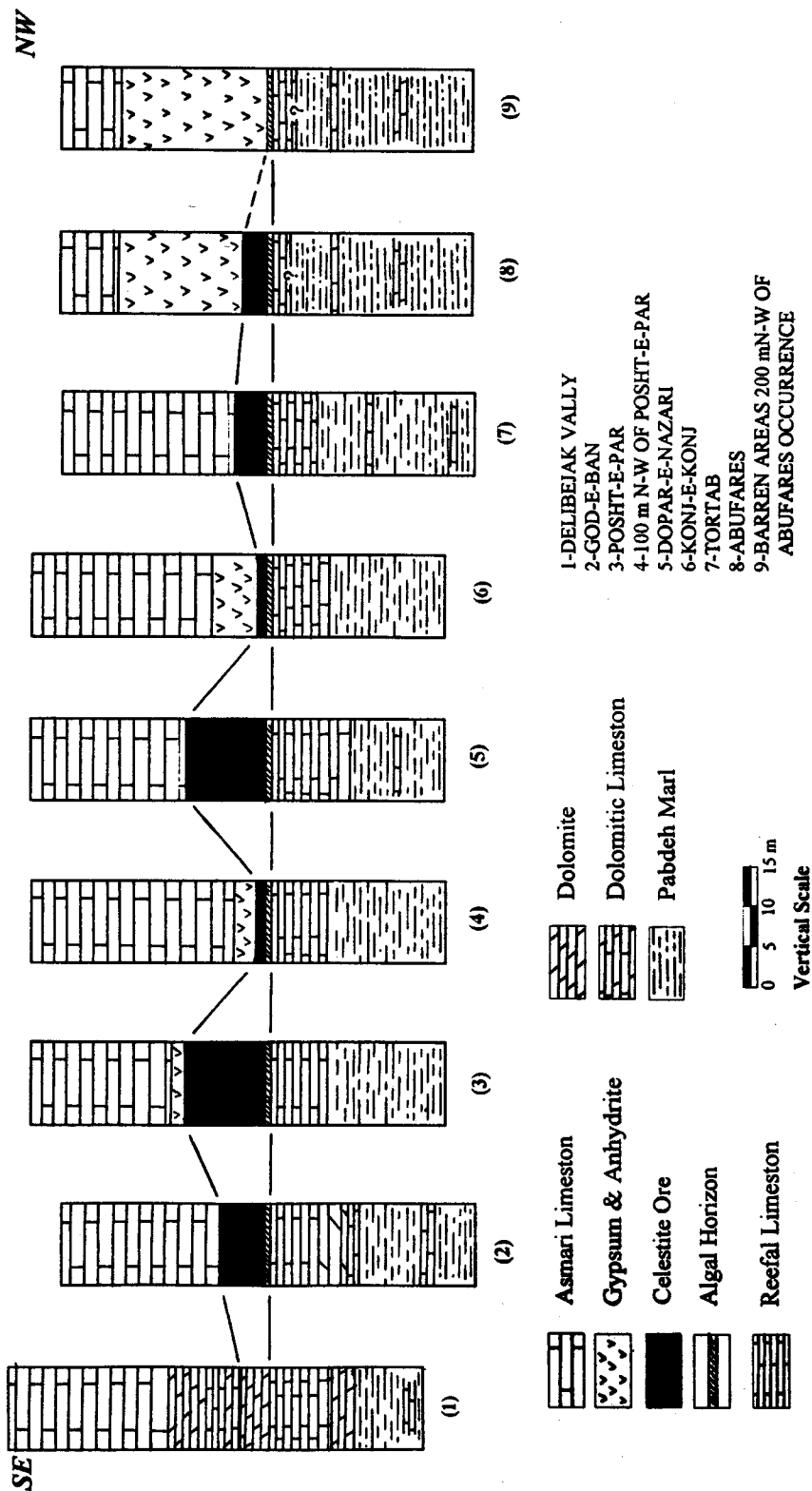


Figure 3. Stratigraphic sections taken in various parts of the Bangestan anticline showing the position of the celestite horizon in the southern flank of this anticline. Columns 2-6 are partly modified from Sabzei [18].

SE

NW

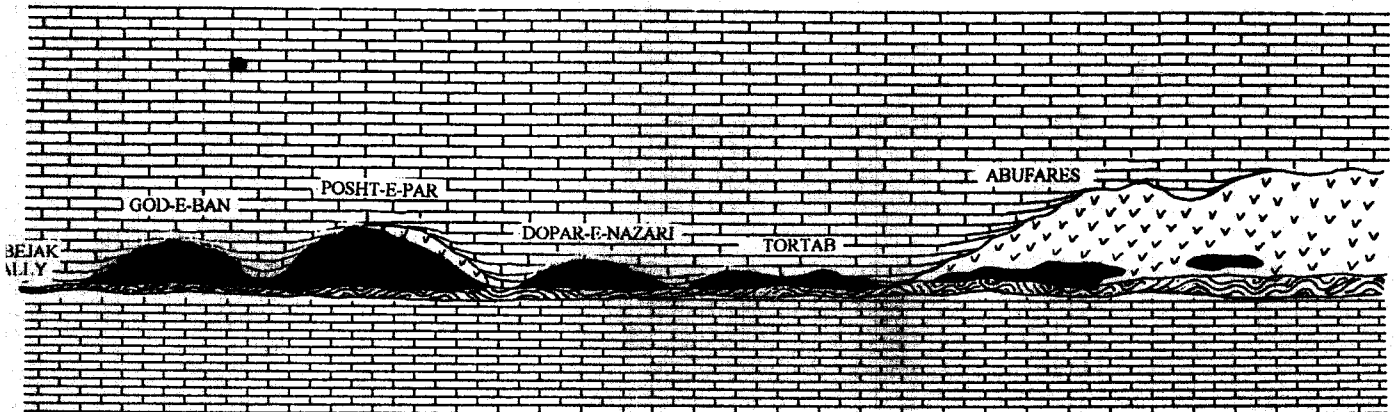


Figure 4. A schematic sketch showing the relationship between celestite concretions and surrounding stratigraphic units

tectonic activity in Holocene are probably responsible for the formation of the Bangestan anticline and other folds and faults in the area.

#### Stratigraphy of the Celestite Horizon

Deposition of celestite is confined to the evaporitic basal unit of Asmari Formation. A similar unit known as Kalhour Member is well developed in southwest Lurestan province northwest of the study area [29], but towards the northeast, the Kalhour member interfingers with calcareous sections of the Asmari Formation and disappears. It is not known if the observed basal evaporitic unit of Asmari Formation and the associated celestite in Bangestan anticline is the southeastern extension of Kalhour Member.

Celestite occurs as very thin layers in Posht-Taveh Olia sandwiched between a reefal limestone and argillaceous limestone (Fig. 1) and extends northward for some 37 km in the form of discontinuous concretions of varying thickness within the same lithologic units. The maximum thickness of the concretions can be seen in the Posht-e-Par area where it exceeds eight meters.

Figure 3 presents 10 stratigraphic sections taken in various parts of the Bangestan anticline showing the position of the celestite bearing horizon in the southern flank of this anticline. It can be seen that in all sections the celestite bearing horizon conformably overlies an algal dolomitic limestone and underlies evaporites or calcareous sections of Asmari Formation. The algal limestone is a thin layer ranging in thickness between 5 and 50 centimeters. Immediately below this unit, a reefal limestone containing large molluscan fragments is present. Due to greater resistance to differential erosion, the reefal limestone stands from the surrounding layers and as it is consistently present under the algal unit and also because it is easily recognized, it was used as an marker bed for tracing the

celestite horizon. Celestite is not present north of AbuFares area (Figure 1) and its position is occupied by an evaporitic layer consisting mainly of gypsum and anhydrite. In many other places the celestite concretions are also seen to be replaced laterally and upwardly by this gypsum layer. Figure 4 is a schematic representation of the relation between these stratigraphic units.

Celestite concretions show great diversity in shape, texture and purity. Southeast of Posht-Taveh Olia, the position of the celestite bearing horizon is occupied by a dolomitic limestone. This bed is best exposed in Delibejak valley (Fig. 1) where it repeats itself in a short distance by local faulting. Apart from large celestite concretions, numerous small displasive and replasive celestite nodules also occur in the overlying gypsum and anhydrite and the underlying algal and reefal limestones. Such nodules are best seen in the AbuFares area. The large molluscan fragments and fossil shells of the underlying reefal limestone show evidence of replacement by celestite (Fig. 5). There is very little doubt that such replacement is the result of diagenetic remobilization of strontium.

#### Ore Mineralogy and Petrography

Diagenetic crystallization rhythmites characterized by alternate layers of fine and coarse grained crystals of celestite are ubiquitous. Amstutz [2] suggests that such rhythmites represent different generations of diagenetic crystallization. This secondary crystallization in many instances completely obliterates the primary texture of the celestite and the algal structure. In this respect, celestite of the Bangestan anticline is very similar to that of the Huitrin formation in Argentina [4].

Macroscopic and microscopic examination of the rhythmites reveals at least three different generations of celestite. The first generation is characterized by fine to



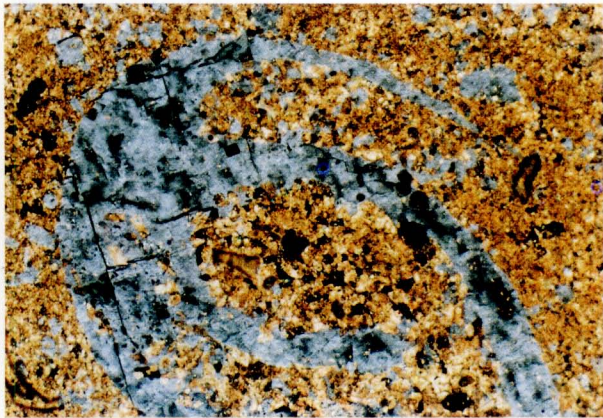


Figure 5. Replacement of large molluskan fragments and fossil shells by celestite

medium grained anhedral crystals darkened by the presence of numerous inclusions.

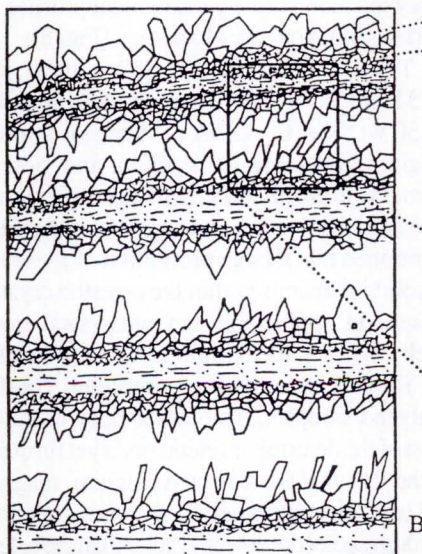
The second generation, which grew directly on top of the first, is characterized by medium to coarse grained subhedral crystals. The second generation crystals are clearer than the first generation crystals because they contain fewer solid and liquid inclusions. Some crystals of the second generation are distinctly zoned. The third generation is seldom present, but when it is, it appears as coarse grained xenomorphic crystals filling the space between the two symmetrically grown bands of the second generation. The third generation crystals are very clear and a paucity of inclusions is noticeable. Figure 6 is a schematic drawing and a photograph of diagenetic rhythmities in the Bangestan anticline.

The reefal dolomitic limestone has a microscopic



3rd generation  
2nd generation  
1st generation

A



B



1st generation  
2nd generation  
3rd generation

C

Figure 6. A photograph (A) and schematic drawing (B and C) of diagenetic crystalization rhythmities in the Bangestan anticline.



oobiomicrosparitic to biosparitic texture in which recrystallized calcite and celestite occur in the center of oolites (Fig. 7). The texture of the algal unit is dolosparitic with microsparitic patches and oolitic structures. It is very rich in the algae remains of the Cyanophyceae family [26]. The celestite horizon displays a holocrystalline sparitic texture. In some concretions, fine grained micritic and

microsparitic crystals are surrounded by coarse sparitic crystals. There is also some intergrowth of dolomite crystals. The presence of abundant solid inclusions of calcite, dolomite and anhydrite in large celestite crystals indicate that the sparitic celestite grew from a fine grained matrix during diagenesis.

Because no barium phases were identified optically it was thought that either the barium minerals were present in cryptocrystalline form escaping microscopic identification, or that some barite was mistakenly identified as celestite because the two minerals exhibit very similar optical properties and are difficult to distinguish under the microscope. However, a lack of detectable barium in chemical analyses (next section) confirmed the absence of barite and other barium phases. This will greatly enhance the commercial quality of the celestite, because commercial celestite should not contain more than 2 weight percent  $BaSO_4$ .

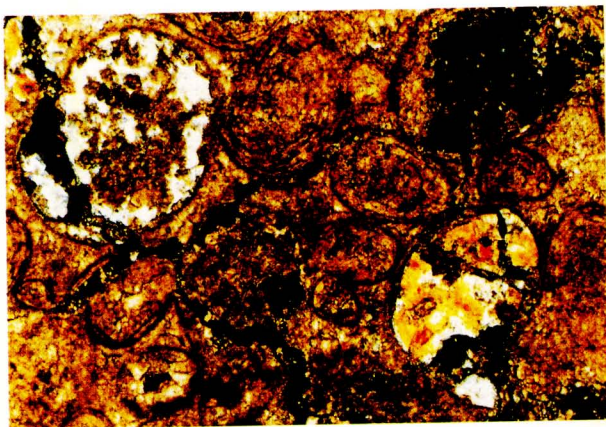


Figure 7. Occurrence of recrystallized calcite and celestite in the center of oolites in oobiomicrosparitic dolomitic limestone (Cross Nicol-40)

### Chemistry of the Ore

Table 1 presents twelve analyses of the ore collected from God-e-Ban (CS1-CS8), Tortab (CS9 & CS10), and AbuFares (CS11 & CS12) occurrences. The elements were determined using standard wet chemical methods [18]. Strontium was measured by both emission and absorption methods and as the results were in good agreement, the reported values are averages of the two measurements. Care was taken to analyse the most representative samples, thus, each analysis represents a number of randomly collected specimens within an interval which were then crushed and quartered in three different stages before taking an aliquot for analysis. Furthermore, in order to investigate systematic variation in elemental composition, samples were systematically collected and analyzed along three geochemical profiles at God-e-Ban, Tortab, and AbuFares localities (Fig. 8).

Table 1 indicates that SrO content varies between 44.51 and 54.89 weight percent, corresponding to 84.68 to 97.30 wt.%  $SrSO_4$ . Other elements of importance include calcium, magnesium, sodium and potassium. These elements probably reflect the presence of minor amounts of calcite, dolomite, gypsum and anhydrite. It must be mentioned that a large proportion of these minerals occur as solid inclusions within the celestite crystals. Iron is not present in appreciable amounts (total iron <0.1 wt%). Lack of detectable barium is also noticeable.

Table 2 presents the correlation coefficients of the analyzed samples. The rather poor correlation between most of the determined elements is yet further confirmation of the fact that the detected calcium, magnesium, alkalis and iron are contributed by the numerous solid inclusions inside the celestite crystals rather than the celestite structure. However, the elemental distribution pattern is clearer in

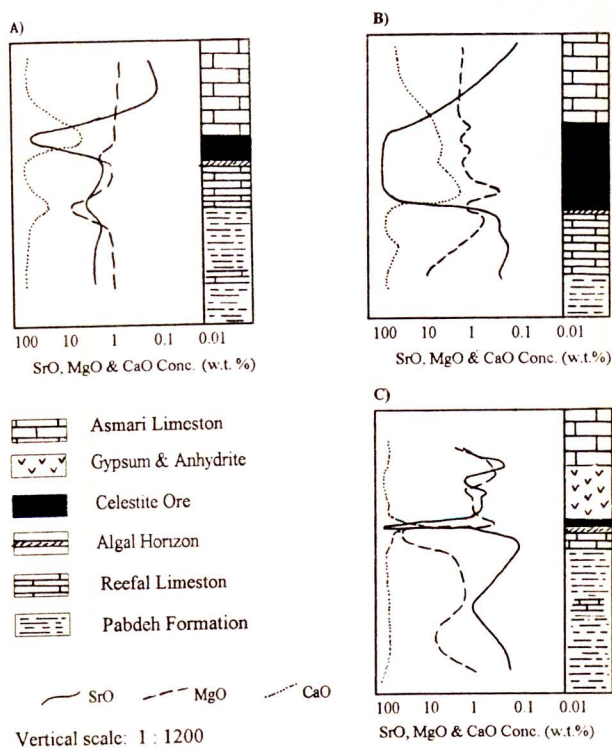


Figure 8. Three geochemical profiles at A: God-e-Ban, B: Tortab and C: Abu Fares Occurrences

**Table 1.** Chemical composition of celestite ore from God-e-ban (CS1-CS8), Tortab (CS9 & CS10), and AbuFares (CS11 & CS12). Detection limit for Ba is 10 ppm

Element Sample No.	SrO wt. %	CaO wt. %	Na <sub>2</sub> O wt. %	K <sub>2</sub> O wt. %	MgO wt. %	Fe <sub>2</sub> O <sub>3</sub> wt. %	BaO wt. %
CS1	51.80	2.70	0.81	0.11	1.06	0.09	n.d
CS2	54.89	0.70	0.92	0.12	0.07	0.07	n.d
CS3	52.68	1.47	0.76	0.10	0.63	0.07	n.d
CS4	51.70	2.24	0.93	0.09	0.90	0.03	n.d
CS5	49.34	5.43	0.70	0.08	1.16	0.07	n.d
CS6	52.98	2.06	0.73	0.06	0.52	0.04	n.d
CS7	48.38	3.09	0.80	0.08	1.71	0.07	n.d
CS8	51.63	3.49	0.83	0.07	0.44	0.06	n.d
CS9	44.51	2.21	0.12	0.12	0.41	0.08	n.d
CS10	53.34	1.94	0.18	0.10	0.62	0.05	n.d
CS11	47.76	5.06	0.05	0.06	0.21	0.05	n.d
CS12	51.19	2.55	0.04	0.09	0.15	0.03	n.d

**Table 2.** Correlation coefficient of celestite ore constituents. Values with confidence level above 95% are considered significant

Elements	SrO	CaO	Na <sub>2</sub> O	K <sub>2</sub> O	MgO
CaO	-0.9302922				
Na <sub>2</sub> O	0.30711	-0.5685943			
K <sub>2</sub> O	0.6940994	-0.3816498	0.9773555		
MgO	-0.9859378	0.9785104	-0.7259971	-0.564038	
Fe <sub>2</sub> O <sub>3</sub>	-0.7198792	0.924307	-0.2116037	0.329152E-8	0.8257489

the geochemical profiles (Fig. 8).

In all profiles, as the celestite concretions are approached and the amount of strontium increases, calcium, magnesium and iron sharply decrease in amount. The behaviour of magnesium is particularly interesting in this respect. Dolomization of aragonite, and to some extent calcite, and the resultant expulsion of strontium ion from the structure is generally advocated by geochemists as a likely source for the contribution of strontium ion to the depositional environment [31]. However, the reverse relationship between magnesium and strontium indicates that dolomization cannot explain the source of strontium in the study area.

The slight increase in the sodium content is also noticeable. According to Muller [22], strontium sulfate deposition from average sea water in coastal lagoons and sabkhas begins at the boundary between calcium carbonate

and calcium sulfate precipitation when the concentration of sea water reaches approximately one fourth of its original volume. The higher sodium content of the celestite horizon compared with the calcareous marker bed also supports a reduction in the volume of the lagoonal brine and resultant increase in salinity. Potassium does not show any definable relationship with strontium variations and because no iron mineral was encountered in the profiles, the decrease in the amount of iron merely reflects the increasing percentage of celestite near the concretions. The absence of detectable barium indicates that the celestite is the end member celestite in the barite-celestite solid solution series. According to Wood and Shaw [31] and Scholle [28], such a celestite precipitates from solutions in which the Sr/Ba ratio is 1500 times the ratio of normal sea water.



**Geothermometry and Isotopic Composition**

Several doubly polished wafers were prepared from the collected samples using mount resin and thin section methods [8,14,24]. The microthermometric studies were made with a Linkam HFS91 combined heating and freezing stage. Furthermore, eight specimens, representing all occurrences, were sent to the University of London (Imperial College) for Fourier Transform Infrared microscopic investigations (FTIR). An additional three samples from God-e-Ban, Posht-e-Par and AbuFares occurrences were sent to Guttingen University for the determination of strontium isotope composition.

Because the majority of fluid inclusions are smaller than 20 microns in diameter, they posed problems in FTIR investigations. However, when the liquid fraction of the inclusions was subjected to ultraviolet radiation in the range of 365 nm, the majority of the inclusions yielded yellow and orange fluorescent light indicative of an immature oil. After heating the samples to the temperature of oil maturity, the released alkane phase yielded a light blue fluorescent light suggesting the presence of a gaseous phase. Attempts to identify the hydrocarbons were not successful because of the small size of the inclusions.

The small size of fluid inclusions also posed serious problems during microthermometric measurements. The majority of the inclusions are two phase liquid and vapour inclusions with a very small bubble. Monophase liquid inclusions are also abundant. A few inclusions containing an unknown daughter phase were also encountered. The lack of inclusions of solitary nature or inclusions that could be related to crystal faces or growth zones made it extremely difficult to discriminate between different generations of inclusions. This is probably partly responsible for the rather

wide range of the homogenization temperatures obtained for the inclusions (Fig. 9). However, the population of inclusions, with homogenization temperatures ranging between 120° and 255°C and a prominent peak at 180°C, probably reflects the most important thermal event to which the ore was subjected.

A plot of the <sup>87</sup>Sr/<sup>86</sup>Sr isotope ratio versus geologic time [10,20] indicates that the bulk of the strontium was provided by Tertiary sea water (Fig. 10). However, the slight enrichment of the obtained values may indicate some supply of Sr from other sources such as the dolomitization of aragonitic limestones, the conversion of anhydrite to gypsum or even contamination by continental groundwater.

**Conclusion**

Field, petrographic and geochemical data all confirm that the formation of celestite concretions at the base of Asmari Formation in the Bangestan anticline is directly related to the deposition of marine evaporites in small, restricted, hypersaline basins along the paleocoast of the Tertiary sea. This is in accordance with Kinsman [19], Butler [6], Greensmith [13], Olausen (1981), and Brodtkorb *et al.* [5], who have successfully demonstrated that celestite normally forms in the subtidal to supratidal facies of the sabkhas, coastal lagoons and salt pans.

According to Berberian and King [3] and Darvishzadeh [9], the Zagros sedimentary basin experienced several regressive and transgressive events in Pale-Oligocene time. In the Oligocene time, most of interior Fars, northwest Lurestan and the Persian Gulf were above sea level, but a major transgression in the late Oligocene and early Miocene epochs resulted in the deposition of Asmari Formation [1].

Close investigation of facies changes in the Bangestan

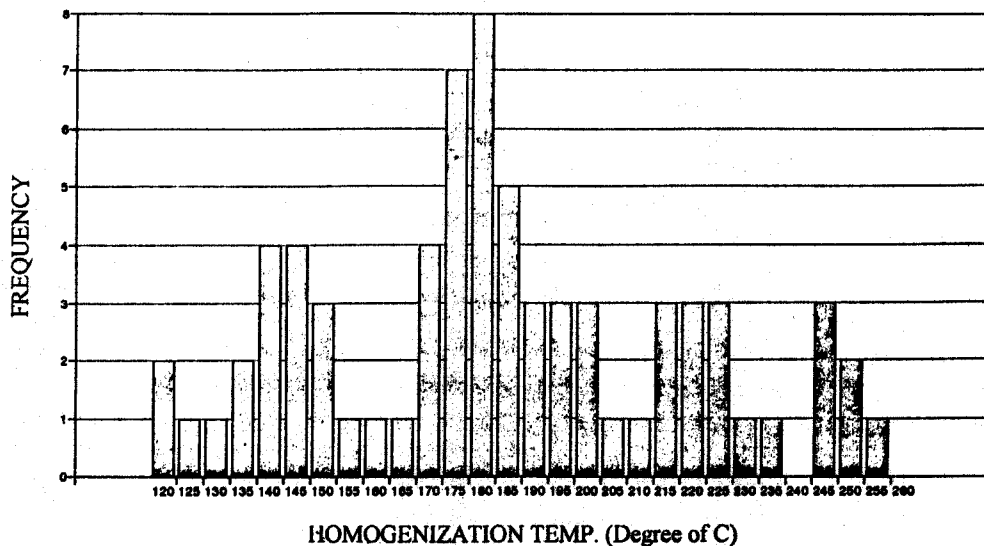


Figure 9. Homogenization Temperature of fluid inclusions in celestite Ore (in degrees C.)

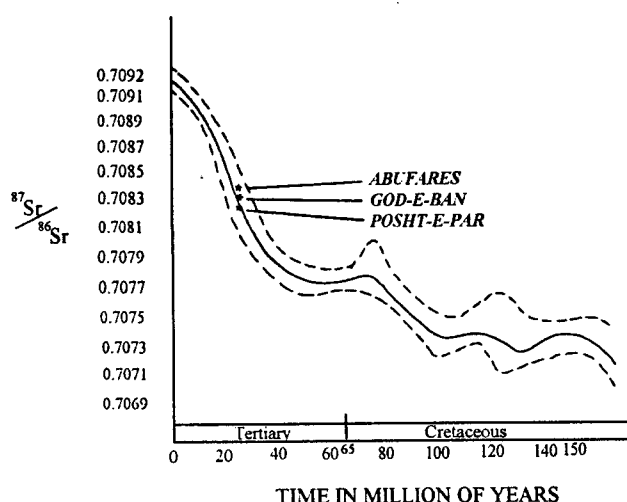


Figure 10.  $^{87}\text{Sr}/^{86}\text{Sr}$  isotope ratio of three celestite samples from Bangestan anticline

anticline reveals that at the time of Asmari Formation deposition, two different sedimentary environments prevailed northwest and southeast of Posht-Taveh Olia. That is, while celestite and gypsum were being precipitated in an intrasupratidal to supratidal environment northwest of Posht-Taveh Olia, an oolitic limestone with oomicropartic to sparitic texture was being deposited in the deeper intratidal to supratidal facies southeast of Posht-Taveh Olia. Figure 11 shows the various sedimentary environments and facies of the Bangestan anticline at the time of celestite deposition i.e. in the late Oligocene and early Miocene epochs. A shallowing-upward sequence is clearly discernible.

Diagenetic recrystallization has obscured and in most cases has completely obliterated the original texture. However, it can readily be demonstrated that large euhedral crystals of celestite have grown from a fine grained celestite matrix (mud).

Extensive dolomitization of the carbonates in the vicinity of Delibejak valley is also of interest. This dolomite appears to be penecontemporaneous as it is restricted to the area adjacent to evaporite deposition. The dolomite is finely crystalline and contains many inclusions, both features typical of modern sabkha or shallow reflux dolomites [11, 15]. Hence, it seems likely that sabkha or reflux processes involving Mg-rich brines were responsible for dolomitization.

The most probable source of strontium, as indicated by the isotopic composition, was Tertiary sea water. In this regard, celestite deposition and the observed strontium anomalies could have occurred in any of the following ways:

1- Direct precipitation of celestite from concentrated brines in a sabkha and supratidal evaporitic environment.

2- Enrichment of interstitial brines in strontium as a result of its expulsion from aragonite structure as it converts to calcite or dolomite in the process of dolomitization.

3- Post diagenetic conversion of primary anhydrites (formed in sabkhas) to gypsum and the resultant expulsion of strontium from anhydrite structure.

Although most of the evidence points to direct precipitation from concentrated brines as being the principal reason for the formation of celestite concretion at the Bangestan anticline, the presence of numerous crystals of celestite in the overlying gypsum layers and the occurrence of intense dolomitization in the vicinity of Delibejak Valley indicate that the other two processes contributed to the formation of these concretions. However, the small number of strontium isotopic data and the absence of C, O, and S isotopic data make it difficult to determine the ultimate source of strontium or the extent of contribution from different sources.

When compared with the overlying Likak deposit or Nakhjir deposit of central Iran, celestite deposition at the base of Asmari Formation may not, as yet, be of great economic importance. However, preliminary assessment of tonnage and grade based on visual evaluation of outcropping mineralization and scattered chip sample analyses indicate that the reserve could be appreciable and must be regarded as a resource for the future, especially considering the extensive development of celestite deposit at the basal unit in Lurestan region.

### Acknowledgements

The authors would like to express their gratitude to the research council of Shiraz University for financial support. Thanks are also extended to Dr. Mick Moser of the University of London for FTIR analyses and to Drs. Hansen and Hiegan of Guttingen University for their help in strontium isotope studies.

### References

1. Alavi, M. Tectonostratigraphic evolution to the Zagros sides of Iran. *Geology*, **8**, 144-149, (1980).
2. Amstutz, G.C. Syngene und epigene in petrographie und lagerstättenkunde. *Schweiz. Min. Petr. Mitt.*, **39**, (H.1), 1-84, (1977).
3. Berberian, M and King, G.C.P., Towards a paleogeography and tectonic evolution of Iran, *Canadian Journal of Earth Sciences*, **18**, (2), 210-265, (1981).
4. Brodtkorb, M.K. Celestite: worldwide classical ore fields. In *Nonmetalliferous stratabound ore fields*, 332 p., Van Nostrand Reinhold, (1989).
5. Brodtkorb, M.K., Ramos, V., Barbieri, M., and Ametrano, S., The evaporitic Celestite-Barite deposits of Neuquen, Argentina, *Mineralium Deposita*, **17**, 423-436, (1982).
6. Butler, G.P., "Strontium geochemistry of modern and

- ancient calcium sulphate minerals", in the Persian Gulf, Ed. by B.H. Purser, 423-452, Springer-Verlag, (1973).
7. Chabou-Mostefai, S., Devolve, J.J., Fuchs, Y., Menant, G. and Riviere, M. Sur les niveaux a celestite de Tunisie centrale et du Sud constatinois. *Sc. de la Terre*, XXII, (3), 291-300, (1978).
  8. Craig, J.R. and Vaughan, D.J., Ore Microscopy and Ore Petrography, John willy. New york, 406 p. (1981).
  9. Darvishzadeh, A. *Geology of Iran*. Amir Kabir Publ., pp. 901, (1992).
  10. DePaolo, D.J. and Ingram, B.L. High resolution stratigraphy with strontium isotopes. *Sciences Col.*, 227, 938-941, (1985).
  11. Evans, G. and Shearman, D.J. Recent celestite from sediments of the Trucial coast of the Persian Gulf. *Nature*, 202, 385-386, (1963).
  12. Falcon, N.L., Southern Iran: Zagros Mountains, in Mesozoic-Cenozoic orogenic belt, *Geol. Soc. London, Spec. Pub.*, 199-211, (1974).
  13. Greensmith J.T., Petrology of the sedimentary rocks, 241 P., George Allen & Unwin LTD., (1981).
  14. Holland, R.A.G., Bruy, C.J. and Spooner, E.T.C., A method for the preparing doubly polished thin section suitable for microthermometric examination of fluid inclusions, *Min. Mag.*, 42, 407-408, (1978).
  15. Illing, L. and Taylor, J.C.M. Penecontemporaneous dolomitization in sabkha Faishakh, Qatar: Evidence from changes in the chemistry of the interstitial brines. *Jour. Sedi. Petr.*, 63, (6), 1042-1048, (1993).
  16. James, G.A. and Wynd, J. C. Stratigraphic nomenclature of Iranian oil consortium agreement area. *AAPG Bull.*, 49, (12), 2182-2245, (1965).
  17. Jami, M. Geology, geochemistry and genesis of the celestite bearing horizon in the Bahmai region, Kohkiloye-Boyer-Ahmad province. MSc Thesis, Geol. Dept. of Shiraz Univ., Iran, (1991). (In Persian).
  18. Jeffrey, P.G. and Hutchison, D., Chemical methods of rock analysis, Pergamon Press, 379 P. (1983).
  19. Kinsman, D.J.J. Modes of formation, sedimentary association and diagnostic features of shallow-water and supratidal evaporite. *AAPG Bull.*, 53, 838-840, (1962).
  20. Koepnick, et al., Construction of the sea water  $87\text{Sr}/86\text{Sr}$  curve for the Cenozoic and Cretaceous. *Chem. Geol.*, 56, 55-81, (1985).
  21. *Mineral Year Book*. U.S. Bureau of Mines, U.S. Department of the Interior, Vol. 1, (1993).
  22. Muller, G. Zur geochemie des strontiums in ozeanen evaporiten unter besonderer berucksichtigung der sedimentaren coelestin-lagerstafte von Hemmelte-West. *Geol. Beiheft*, 35 1-90, (1962).
  23. Ramos, V.A. and De-Brodtkorb, M.K. Celestite, barite, magnesite and fluorspar: stratabound setting through time and space. In *Nonmetalliferous stratabound ore fields*, pp. 297-321. Van Nostrand Reinhold, (1989).
  24. Roedder, E. *Fluid inclusions, reviews in mineralogy*, Vol. 12, p. 645. Mineralogical Society of America, (1984).
  25. Romankov, I.F., Moomenzadeh, M., Mogarovsky, V.V. and Kakorin, V.K. New celestite bearing zone, east of Mediterranean sea (Zagros mountains, SW of Iran). *Geological Survey of Iran, Internal Report*, (1988). (In Russian).
  26. Sabzei, M. Celestite prospecting in Bangestan anticline. Ministry of Mines and Metals, Kohkiloye and BoyerAhmad province, p. 65. Internal Report, (1990). (In Persian).
  27. Schiebel, W. A new strontium deposit in Iran. *London Ind. Miner.*, 132, 54-59, (1978).
  28. Scholle, P.A., Stemmerik, L. and Harpoth, O. Origin of major karst-associated celestite mineralization in karstryggen, central east Greenland. *Jour. Sed. Petrology*, 60, (3), 397-410, (1990).
  29. Stocklin, J. Structural history and tectonics of Iran. *AAPG Bull.*, 52, 1229-1258, (1968).
  30. Stocklin, J. Stratigraphic Lexicon of Iran. *Geol. Survey of Iran, Rep. No. 18*, p. 384, (1974).
  31. Wood, M.W. and Shaw, H.F. The geochemistry of celestites from the Yate area near Bristol (U.K.), *Chemical Geology*, 17, 179-193, (1976).